Exact solution of Boltzmann equation in a longitudinal expanding system

Shile Chen[*] and Shuzhe Shi[†]
Department of Physics, Tsinghua University, Beijing 100084, China

Analytical solutions to the microscopic Boltzmann equation are useful in testing the applicability and accuracy of macroscopic hydrodynamic theory. In this work, we present exact solutions of the relativistic Boltzmann equation, based on a new family of exact solutions of the relativistic ideal hydrodynamic equations [S. Shi, S. Jeon, and C. Gale, Phys. Rev. C **105**, L021902 (2022)]. To the best of our knowledge, this is the first exact solution that allows longitudinal expansion with broken boost invariance.

Introduction. Hydrodynamics is a macroscopic, long-wavelength effective theory that describes the collective motions in many-body systems. The commonly used framework of relativistic hydrodynamic equations is derived from the microscopic Boltzmann equations by taking different approximations, such as the relaxation time approximation [1], Chapman–Enskog expansion [2,3], and moment expansion based methods by Isreal and Stewart [4] and by Denicol *et al.* [5–7]. In these derivations, the systems are assumed to be close to local equilibrium, and the distribution function is the thermal equilibrium one plus small derivations expanded in different bases. The hydrodynamic theory only keeps lower order moments in the Knudsen expansion, leaving the higher order ones either truncated out or extrapolated under certain assumptions. Therefore, it is traditionally expected to be applicable in near-equilibrium systems with a small Knudsen number.

The success of applying hydrodynamic theory in describing the final state observables of collective motion in high energy nucleus-nucleus, proton-nucleus, and even proton-proton collisions (see, e.g., [8–11]) has drawn significant interests in discussions of relieving the assumptions for the applicability of hydrodynamics [12–30]. A crucial step is to compare the hydro results to those of the Boltzmann equation, which describes the evolution of the microscopic particle distribution.

Taking the general form in a curvilinear coordinates, the Boltzmann equation for on-shell distribution function reads (see, e.g., [31–33])

$$\left(p^\mu \partial_\mu + \Gamma^\rho{}_{\mu\nu} p^\mu p_\rho \frac{\partial}{\partial p_\nu} \right) f(x^\alpha, p_\beta) = \mathcal{C}[f],$$

$$\mathcal{C}[f] = \frac{p_\mu u^\mu(x)}{\tau_r(x)} (f(x^\alpha, p_\beta) - f_{\text{eq}}(x^\alpha, p_\beta)), \quad (1)$$

*csl2023@tsinghua.edu.cn
†shuzhe-shi@tsinghua.edu.cn

where we have taken the relaxation time approximation (RTA) [1] for the collisions kernel. The Christoffel symbol is given by $\Gamma^\rho{}_{\mu\nu} = \frac{g^{\rho\gamma}}{2}(\frac{\partial g_{\gamma\mu}}{\partial x^\nu} + \frac{\partial g_{\gamma\nu}}{\partial x^\mu} - \frac{\partial g_{\mu\nu}}{\partial x^\gamma})$, with $g^{\mu\nu}$ being the metric. Taking the conformal limit that $m = 0$, the relaxation time reads $\tau_r(\hat{x}) = 5\bar{\eta}/\hat{T}(\hat{x})$, and $\bar{\eta}$ is the shear viscosity to entropy ratio [5,6,34,35]. The local equilibrium distribution function is assumed to be of Boltzmann form, $f_{\text{eq}} = \exp(-\hat{p}_\mu \hat{u}^\mu/\hat{T})$. For the distribution functions in Eq. (1), all momentum arguments are covariant and coordinate arguments are contravariant. $\hat{T}(\hat{x})$ and $\hat{u}^\mu(\hat{x})$ are respectively the space-time dependent temperature and velocity. The space-time profiles of $\hat{T}$ and $\hat{u}^\mu$ are not arbitrary: they are constrained by continuity relations such as hydrodynamics.

In a given coordinate system, if one makes certain assumptions such that the Boltzmann equation can be expressed in a form without the derivatives with respect to the spatial coordinates and momenta, there exists a formal solution [34–36]. With explicit form which will be shown later in the main text, the formal solution depends only on the temporal coordinate and is homogeneous with respect to the spatial one. The nontrivial spatial expansion can be introduced if one takes a coordinate of a comoving frame of a known solution to the hydrodynamic equations [37–40]. A family of exact solutions for ideal fluids, found recently in [41], is homogeneous in the transverse plane and allows expansion—either symmetric or asymmetric—in the longitudinal direction, which breaks the boost invariance. In this work, we find the comoving frame of the new solution and construct the formal solution accordingly. We then compute the hydrodynamics quantities and analyze how they relax to the hydro limit.

Comoving frame of the longitudinal expanding flow. Taking the general form in a curvilinear coordinates, the hydrodynamic equation reads

$$\mathcal{D}_\mu T^{\mu\nu} \equiv \partial_\mu T^{\mu\nu} + \Gamma^\mu{}_{\rho\mu} T^{\rho\nu} + \Gamma^\nu{}_{\rho\mu} T^{\rho\mu} = 0, \quad (2)$$

where $T^{\mu\nu}$ is the energy-momentum tensor and $\mathcal{D}_\mu$ is the covariant derivative. In Ref. [41], a family of exact solutions

for longitudinally expanding ideal fluids was found,

$$\frac{T_{\text{ideal}}}{T_i} = \left(\frac{t_0}{\tau_i} + \frac{a_{NN}\tau e^\eta}{\tau_i}\right)^{\frac{1-c_s^2}{4}\frac{1}{a^2} - \frac{1+c_s^2}{4}}$$

$$\times \left(\frac{t_0}{\tau_i} + \frac{\tau e^{-\eta}}{a_{NN}\tau_i}\right)^{\frac{1-c_s^2}{4}a^2 - \frac{1+c_s^2}{4}},$$

$$u^\tau = \frac{1}{2}\left(\sqrt{\frac{t_0 e^{-\eta} + \tau a}{t_0 e^\eta + \tau/a}} + \sqrt{\frac{t_0 e^\eta + \tau/a}{t_0 e^{-\eta} + \tau a}}\right), \qquad (3)$$

$$u^\eta = \frac{1}{2\tau}\left(\sqrt{\frac{t_0 e^{-\eta} + \tau a}{t_0 e^\eta + \tau/a}} - \sqrt{\frac{t_0 e^\eta + \tau/a}{t_0 e^{-\eta} + \tau a}}\right).$$

In the solution, τ and η are the proper time and rapidity in Milne coordinates, respectively. c_s is the speed of sound, a is a dimensionless parameter characterizing the asymmetry between forward and backward rapidity range, and T_i and τ_i are positive constants that respectively scale the temperature and time. The non-negative time constant t_0 serves as a translation of the Minkowski time, and it corresponds to the time needed for the colliding nuclear pancakes to pass through each other in relativistic heavy-ion collisions [41]. Focusing on the central rapidity slice for a reflectional symmetric system ($a = 0$), the temperature decreases as $T(\tau) = T_i \left(\frac{\tau_i}{\tau + t_0}\right)^{\frac{1}{3}}$, which decays slower than the Bjorken flow at small τ and approaches the Bjorken limit when $\tau \gg t_0$.

In this work, we introduce a new coordinate system which can be transformed from the Milne coordinates

$$\hat{x}^0 = \frac{2a\,\tau_i}{1+a^2}\left[\left(\frac{t_0 + a\,\tau e^\eta}{\tau_i}\right)^{\frac{1}{a}}\left(\frac{t_0}{\tau_i} + \frac{\tau e^{-\eta}}{a\,\tau_i}\right)^a\right]^{\frac{1+a^2}{4a}},$$

$$\hat{x}^1 = \frac{1+a^2}{4a}\ln\left[\left(\frac{t_0 + a\,\tau e^\eta}{\tau_i}\right)^{\frac{1}{a}} \Big/ \left(\frac{t_0}{\tau_i} + \frac{\tau e^{-\eta}}{a\,\tau_i}\right)^a\right],$$

$$\hat{x}^x = x, \quad \hat{x}^y = y. \qquad (4)$$

The corresponding metric is

$$\hat{g}^{\mu\nu} = \text{diag}[e^{2\frac{1-a^2}{1+a^2}\hat{x}^1}, -(\hat{x}^0)^{-2}e^{2\frac{1-a^2}{1+a^2}\hat{x}^1}, -1, -1], \qquad (5)$$

and the nonvanishing components of the Christoffel symbol are

$$\hat{\Gamma}^0_{11} = \hat{x}^0, \quad \hat{\Gamma}^1_{10} = \hat{\Gamma}^1_{01} = \frac{1}{\hat{x}^0},$$

$$\hat{\Gamma}^0_{01} = \hat{\Gamma}^0_{10} = \hat{\Gamma}^1_{11} = (\hat{x}^0)^2\hat{\Gamma}^1_{00} = \frac{a^2-1}{a^2+1}. \qquad (6)$$

From now on, we use the "hat" ($\hat{\cdot}$) notation to denote quantities under the new coordinate system (4). Under the comoving frame, the solution (3) becomes "static" such that all spatial components vanish, and the space-time profile of the solution reads

$$\hat{T}_{\text{ideal}} = \sqrt{\hat{g}^{00}}\, T_i\left(\frac{\tau_i}{\hat{x}^0}\right)^{c_s^2},$$

$$\hat{u}^0 = \sqrt{\hat{g}^{00}}, \quad \hat{u}^1 = \hat{u}^x = \hat{u}^y = 0. \qquad (7)$$

Therefore, (4) is the the comoving frame of the asymmetric expanding flow (3). We have redefined T_i to absorb a space-time independent factor.

Taking $t_0 = 0$ and $a = 1$, Eq. (4) returns to the Milne coordinate and Eq. (7) returns to the Bjorken-Hwa solution [42,43]. With general values for t_0 and a, one may still connect the new solution with the Bjorken-Hwa solution by rescaling $\hat{u}^\mu$ and $\hat{T}$ by $(\hat{g}^{00})^{-1/2}$ and replacing $\hat{x}^0$ by τ. $\hat{x}^0$ and $\hat{x}^1$, thus, are respectively referred to as the hat proper time and hat rapidity in this paper.

The Boltzmann equation in the co-moving frame. Noting the simplicity of the solution (7) in the comoving frame (4) and its similarity to the Bjorken-Hwa solution, we take the comoving frame and solve the Boltzmann equations. Following the property of the hydro solution, we focus on the systems that are homogeneous in the transverse plane, and the Boltzmann equation (1) in the comoving frame becomes

$$\left(\hat{g}^{00}\hat{p}_0\frac{\partial}{\partial\hat{x}^0} + \hat{g}^{11}\hat{p}_1\frac{\partial}{\partial\hat{x}^1} + \frac{a^2-1}{a^2+1}(\hat{p}_x^2 + \hat{p}_y^2)\frac{\partial}{\partial\hat{p}_1}\right)f(\hat{x}^\alpha, \hat{p}_\beta)$$

$$= -\frac{\hat{p}_0\hat{u}^0\hat{T}(\hat{x}^0)}{5\bar{\eta}}(f(x^\alpha, \hat{p}_\beta) - f_{\text{eq}}(x^\alpha, \hat{p}_\beta)). \qquad (8)$$

Noting that the solution (3) requires a simple relation between the pressure and the energy density, $P = c_s^2\varepsilon$, which corresponds to the conformal limit in a kinetic theory, we therefore focus on massless particles in this work. The nonvanishing prefactor of the derivative with respect to $\hat{p}_1$ posts challenges in getting exact solution of the Boltzmann equation: the formal solution [34–36] can no longer be applied in such cases. One may try to simplify the coordinate and momentum dependence of the distribution function by analyzing the symmetry properties of the hydro solution (7) and the Boltzmann equation (8). We note that (8) is invariant if one performs a pseudoboost such that $\hat{x}^0 \to \hat{x}^0$, $\hat{x}^1 \to \hat{x}^1 + \eta_b$, and $\hat{x}^i \to \hat{x}^i e^{-\frac{1-a^2}{1+a^2}\eta_b}$ for $i \in \{x, y\}$, which leads to $\hat{g}^{\mu\nu} \to e^{2\frac{1-a^2}{1+a^2}\eta_b}\hat{g}^{\mu\nu}$, and correspondingly, $\hat{p}_T \to \hat{p}_T e^{\frac{1-a^2}{1+a^2}\eta_b}$, $\hat{T} \to \hat{T} e^{\frac{1-a^2}{1+a^2}\eta_b}$, and $\hat{u}^0 \to \hat{u}^0 e^{\frac{1-a^2}{1+a^2}\eta_b}$. Noting that such a transformation scales the transverse coordinates differently than the temporal and longitudinal ones, it simplifies (8) under two special situations. One is to eliminate the $\hat{x}^x$ and $\hat{x}^y$ coordinates; the other is to let $a = 1$ so that the transverse scaling factor ($e^{\frac{1-a^2}{1+a^2}\eta_b}$) is unity. Both simplifications correspond to special solutions of (8) and will be discussed in what follows sequentially.

Solution in $1 + 1D$. First, we consider a coordinate system with only $\hat{x}^0$ and $\hat{x}^1$, i.e., a $1 + 1$ dimensional system. This is equivalent to considering $f \propto \delta(\hat{p}_x)\delta(\hat{p}_y)$ so that momentum derivative in (8) is eliminated. Under such a constraint, the on-shell condition becomes $\hat{p}_0 = |\hat{p}_1|/\hat{x}^0$, and the speed of sound for a massless free particle is $c_s = 1$. We find that both the homogeneous equilibrium distribution and the equivalent relaxation time are independent of $\hat{x}^1$. This further allows us to assume the solution to be independent of the hat rapidity, and Eq. (8) becomes

$$\partial_{\hat{x}^0}f(\hat{x}^0, \hat{p}_1) = -\frac{\hat{T}(\hat{x}^0)}{5\bar{\eta}}\left[f(\hat{x}^0, \hat{p}_1) - \exp\left(-\frac{\hat{p}_0}{\hat{T}(\hat{x}^0)}\right)\right]. \qquad (9)$$

In $1 + 1$D, $\bar{\eta}$ has no physics meaning, but it is a dimensionless parameter that scales the relaxation time. With arbitrary initial distribution function given at hat proper time $\hat{x}_i^0$, $f_i(\hat{x}_i^0, \hat{p}_1)$, based on Landau matching, we find the equation to the effective temperature of $1 + 1$D system,

$$\hat{T}_{\text{eff}}^2(\hat{x}^0) = \frac{(\hat{x}^0)^2}{(\hat{x}_i^0)^2} e^{-\frac{1}{5\bar{\eta}} \int_{\hat{x}_i^0}^{\hat{x}^0} \hat{T}_{\text{eff}}(x') dx'} \hat{T}_0^2$$
$$+ \frac{1}{5\bar{\eta}} \int_{\hat{x}_i^0}^{\hat{x}^0} dx' \frac{(\hat{x}^0)^2}{(\hat{x}')^2} e^{-\frac{1}{5\bar{\eta}} \int_{\hat{x}'}^{\hat{x}^0} \hat{T}_{\text{eff}}(x'') dx''} \hat{T}_{\text{eff}}^3(\hat{x}'). \quad (10)$$

When $\bar{\eta} \to 0$, effective temperature returns to the ideal hydro solution $\hat{T}(\hat{x}^0) = T_i \tau_i / \hat{x}^0$.

It is worth noting that, while $f(\hat{x}^0, \hat{p}_1)$ does not explicitly depend on hat rapidity, the corresponding energy-momentum stress tensor still nontrivially depends on $\hat{x}^1$ via the Jacobian of the momentum integral (i.e., $\sqrt{\hat{g}^{00}}$). In other words, the $\hat{x}^1$ dependence of hydrodynamic quantities can be factored out as scaling constants.

Symmetric solution in $3 + 1$D. Compared to the aforementioned $1 + 1$D solution, the longitudinal distribution of relativistic heavy-ion collisions particle production is better described by solutions in the $3 + 1$ dimensional coordinate [41], even if the transverse profiles are assumed to be homogeneous. It is, thus, important to find solutions of the Boltzmann equation in $3 + 1$D coordinates for realistic studies. When taking into account the transverse degrees of freedom, a solution of the Boltzmann equation (8) can be found only when $a = 1$, which describes systems that are symmetric when reflecting the longitudinal direction. When $a = 1$, the hydro solution (7) is equivalent to the Bjorken-Hwa flow if one performs a mapping between the hat and Milne coordinates, $\hat{x}^0 \leftrightarrow \tau$ and $\hat{x}^1 \leftrightarrow \eta$. Such a mapping is essentially a Minkowski-time translation [41], but it corresponds to nontrivial physics consequence as it gives the correct plateau structure in the rapidity distribution of final state particles which is observed in experiments. The coordinate mapping naturally leads to a corresponding relation between solution to the Boltzmann equation and [40]. The Boltzmann equation takes a simple form,

$$\partial_{\hat{x}^0} f(\hat{x}^0, \hat{p}_\mu) = -\frac{\hat{T}(\hat{x}^0)}{5\bar{\eta}} (f(\hat{x}^0, \hat{p}_\mu) - e^{-\frac{\hat{p}_0(\hat{x}^0)}{\hat{T}(\hat{x}^0)}}), \quad (11)$$

and the formal solution [34–36] is applicable,

$$f(\hat{x}^0, \hat{p}_1, \hat{p}_T) = D(\hat{x}^0, \hat{x}_i^0) f_0(\hat{x}_i^0, \hat{p}_1, \hat{p}_T)$$
$$+ \frac{1}{5\bar{\eta}} \int_{\hat{x}_i^0}^{\hat{x}^0} d\hat{x}' D(\hat{x}^0, \hat{x}') \hat{T}(\hat{x}') e^{-\frac{\hat{p}_0(\hat{x}')}{\hat{T}(\hat{x}')}}. \quad (12)$$

Here, $f_0(\hat{x}_i^0, \hat{p}_1, \hat{p}_T)$ is the initial distribution at hat proper time $\hat{x}_i^0$, $D(\hat{x}^0, \hat{x}_i^0) \equiv \exp\left[-\frac{1}{5\bar{\eta}} \int_{\hat{x}_i^0}^{\hat{x}^0} \hat{T}(\hat{x}') d\hat{x}'\right]$, and the energy is given by the on-shell condition $\hat{p}_0(\hat{x}^0) = \sqrt{(\frac{\hat{p}_1}{\hat{x}^0})^2 + \hat{p}_T^2}$. The temperature is fixed by ensuring energy conservation, $0 = \int d\hat{P}(\hat{p}^0)^2 (f(\hat{x}^0, \hat{p}_\mu) - e^{-\frac{\hat{p}_0}{\hat{T}(\hat{x}^0)}})$, where $\int d\hat{P} \equiv \int \frac{d^4 \hat{p}}{(2\pi)^3 \sqrt{-\hat{g}}} 2\delta((\hat{p}_0)^2 - (\frac{\hat{p}_1}{\hat{x}^0})^2 - \hat{p}_T^2)$ with $\sqrt{-\hat{g}} = \sqrt{-\det \hat{g}_{\mu\nu}} = \hat{x}^0$ and $d^4 \hat{p} = d\hat{p}_0 d\hat{p}_1 d\hat{p}_x d\hat{p}_y$. There

is no simple explicit form for the integral of the solution (12). Nevertheless, we may solve the integral numerically, construct the stress tensor out of the distribution function, extract the macroscopic hydrodynamic quantities, and analyze their "time" evolution.

Hydrodynamic quantities. Given the distribution function, the energy momentum tensor reads

$$\hat{T}^{\mu\nu} = \int d\hat{P} \hat{p}^\mu \hat{p}^\nu f(\hat{x}, \hat{p}). \quad (13)$$

In the conformal limit, the bulk viscosity vanishes, and one can always decompose stress tensor as

$$\hat{T}^{\mu\nu} = \hat{\varepsilon}(\hat{x}) \hat{u}^\mu \hat{u}^\nu + \hat{\Delta}^{\mu\nu} \hat{\mathcal{P}}(\hat{x}) + \hat{\pi}^{\mu\nu}(\hat{x}), \quad (14)$$

where $\hat{\varepsilon}(\hat{x})$ is the energy density, $\hat{\mathcal{P}}(\hat{x})$ the thermodynamic pressure, $\hat{\pi}^{\mu\nu}(\hat{x})$ the shear viscous stress tensor, and $\hat{\Delta}^{\mu\nu} \equiv \hat{g}^{\mu\nu} - \hat{u}^\mu \hat{u}^\nu$ the "space" projection operator. $\hat{\pi}^{\mu\nu}$ is symmetric, traceless ($\hat{g}_{\mu\nu} \hat{\pi}^{\mu\nu} = 0$), and orthogonal to the fluid velocity ($\hat{u}_\mu \hat{\pi}^{\mu\nu} = \hat{u}_\nu \hat{\pi}^{\mu\nu} = 0$). In $3 + 1$D, a conformal system has $c_s = 1/\sqrt{3}$, and the energy density, thermodynamic pressure, and entropy only depend on temperature:

$$\hat{\varepsilon} = \frac{3\hat{T}^4}{\pi^2}, \quad \hat{P} = \frac{\hat{T}^4}{\pi^2}, \quad \hat{s} = \frac{\hat{\varepsilon} + \hat{P}}{\hat{T}} = \frac{4\hat{T}^3}{\pi^2}. \quad (15)$$

Placing $\int d\hat{P} \hat{p}^\mu \hat{p}^\nu$ on both side of Eq. (12), we obtain the integration form of the stress tensor,

$$\hat{T}^{\mu\nu}(\hat{x}^0) = D(\hat{x}^0, \hat{x}_i^0) \mathcal{H}^{\mu\nu}\left(\frac{\hat{x}_i^0}{\hat{x}^0}\right) \int \frac{p^3 dp}{2\pi^2} f_0(\hat{x}_i^0, \hat{p}_1, \hat{p}_T)$$
$$+ \frac{1}{5\bar{\eta}} \int_{\hat{x}_i^0}^{\hat{x}^0} d\hat{x}' D(\hat{x}^0, \hat{x}') \hat{T}(\hat{x}') \mathcal{H}^{\mu\nu}\left(\frac{\hat{x}'}{\hat{x}^0}\right)$$
$$\times \int \frac{p^3 dp}{2\pi^2} f_{\text{eq}}(\hat{x}', \hat{p}_0(\hat{x}')), \quad (16)$$

with nonvanishing elements of tensor $\mathcal{H}^{\mu\nu}$ given by

$$\mathcal{H}^{00}(\xi) \equiv \frac{\xi}{4\pi} \int \frac{\sin\theta \, d\theta \, d\varphi}{(\sin^2\theta + \xi^2 \cos^2\theta)^{-\frac{1}{2}}} = \mathcal{R}(\xi), \quad (17)$$

$$\mathcal{H}^{11}(\xi) \equiv \frac{\xi^3}{4\pi} \frac{1}{(\hat{x}^0)^2} \int \frac{\cos^2\theta \sin\theta \, d\theta \, d\varphi}{(\sin^2\theta + \xi^2 \cos^2\theta)^{\frac{1}{2}}} = \frac{\mathcal{R}^L(\xi)}{(\hat{x}^0)^2},$$
$$(18)$$

$$\mathcal{H}^{xx}(\xi) \equiv \frac{\xi}{4\pi} \int \frac{\sin^2\theta \cos^2\varphi \sin\theta \, d\theta \, d\varphi}{(\sin^2\theta + \xi^2 \cos^2\theta)^{\frac{1}{2}}} = \mathcal{R}^T(\xi), \quad (19)$$

where $\mathcal{R}(\xi) = \frac{\xi}{2}(\xi + \frac{\arccos\xi}{\sqrt{1-\xi^2}})$, $\mathcal{R}^L(\xi) = \frac{\xi^2(\mathcal{R}(\xi) - \xi^2)}{1-\xi^2}$, $\mathcal{R}^T(\xi) = \frac{(1-2\xi^2)\mathcal{R}(\xi) + \xi^4}{2(1-\xi^2)}$, and $\mathcal{H}^{yy}(\xi) = \mathcal{H}^{xx}(\xi)$ [44]. Noting that $\hat{T}^{\mu\nu}$ is always diagonal, the fluid is still "at rest" in the comoving frame, i.e., $\hat{u}^\mu$ in (7) remains the correct velocity decomposition of (16). For a conformal system that is homogeneous in the transverse plane, the stress tensor is traceless ($\hat{g}_{\mu\nu} \hat{T}^{\mu\nu} = 0$) and symmetric when exchanging the transverse variables ($\hat{T}^{xx} = \hat{T}^{yy}$). There remain two independent components in the stress tensor: the effective temperature determined by $\hat{T}^{00} = \frac{3\hat{T}_{\text{eff}}^4}{\pi^2}$, and the shear viscous tensor $\hat{\pi}^{xx} \equiv \hat{T}^{xx} - \frac{\hat{T}^{00}}{3}$.
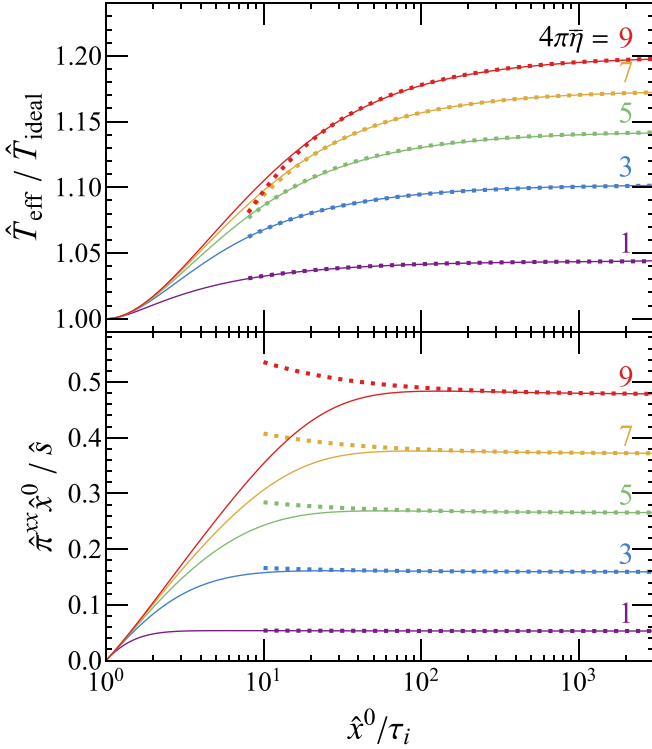
FIG. 1. Scaled temperature (upper) and scaled temperature shear viscous stress tensor (lower) as functions of $\hat{x}^0/\hat{x}_i^0$ obtained by different shear viscosity to entropy ratios ($\bar{\eta}$). Curves are respectively for $\bar{\eta} = 1/4\pi$ (purple), $3/4\pi$ (blue), $5/4\pi$ (green), $7/4\pi$ (yellow), and $9/4\pi$ (red). Dashed curves correspond to the long-time asymptotic solutions (21).

We start the evolution from an equilibrium distribution with temperature denoted by $\hat{T}_0$, and the effective temperature and shear viscous stress tensor read

$$\hat{T}_{\text{eff}}^4(\hat{x}^0) = D(\hat{x}^0, \hat{x}_i^0)\tilde{\mathcal{H}}_0\left(\frac{\hat{x}_i^0}{\hat{x}^0}\right)\hat{T}_0^4$$

$$+ \frac{1}{5\bar{\eta}}\int_{\hat{x}_i^0}^{\hat{x}^0} d\hat{x}' D(\hat{x}^0, \hat{x}')\tilde{\mathcal{H}}_0\left(\frac{\hat{x}'}{\hat{x}^0}\right)\hat{T}_{\text{eff}}^5(\hat{x}'),$$

$$\hat{\pi}^{xx}(\hat{x}^0) = D(\hat{x}^0, \hat{x}_i^0)\tilde{\mathcal{H}}_x\left(\frac{\hat{x}_i^0}{\hat{x}^0}\right)\hat{T}_0^4$$

$$+ \frac{1}{5\bar{\eta}}\int_{\hat{x}_i^0}^{\hat{x}^0} d\hat{x}' D(\hat{x}^0, \hat{x}')\tilde{\mathcal{H}}_x\left(\frac{\hat{x}'}{\hat{x}^0}\right)\hat{T}_{\text{eff}}^5(\hat{x}'), \quad (20)$$

where $\tilde{\mathcal{H}}_0 \equiv \mathcal{H}^{00}$ and $\tilde{\mathcal{H}}_x \equiv \frac{3}{\pi^2}(\mathcal{H}^{xx} - \frac{\mathcal{H}^{00}}{3})$. We therefore look into the dimensionless quantities, scaled temperature $\hat{T}_{\text{eff}}/\hat{T}_{\text{ideal}}$ and scaled shear viscous stress tensor $\hat{x}^0\hat{\pi}^{xx}/\hat{s}$, whose "evolution" with hat proper time are shown in Fig. 1 for various $\bar{\eta}$. The matching condition of the initial state requires that parameters in $\hat{T}_{\text{ideal}}$ shall be taken as $T_i = \hat{T}_0$ and $\tau_i = \hat{x}_i^0$. In making the plot, we have set $\hat{T}_0 = 1/\tau_i$.

In Fig. 1, dashed curves are also shown to indicate the long hat-proper-time asymptotic analytical results obtained from a

perturbative analysis of (20),

$$\frac{\hat{T}_{\text{eff}}}{\hat{T}_{\text{ideal}}} = e_{\bar{\eta}} - \frac{2\bar{\eta}}{3}\left(\frac{\tau_i}{\hat{x}^0}\right)^{\frac{2}{3}} + \mathcal{O}((\hat{x}^0)^{-\frac{4}{3}}),$$

$$\frac{\hat{\pi}^{xx}\hat{x}^0}{\hat{s}} = \frac{2\bar{\eta}}{3} + \frac{40\,\bar{\eta}^2}{63\,e_{\bar{\eta}}\,T_i\,\tau_i}\left(\frac{\tau_i}{\hat{x}^0}\right)^{\frac{2}{3}} + \mathcal{O}((\hat{x}^0)^{-\frac{4}{3}}). \quad (21)$$

Details are shown in the Appendix. Starting from an initial condition which matches the ideal temperature, the scaled temperature first deviates from unity driven by the viscous effect, then it approaches the ideal limit with the effective temperature being $e_{\bar{\eta}}T_i$ at large enough $\hat{x}^0$. $e_{\bar{\eta}}$ is a viscosity-dependent constant that shall be obtained numerically, and it is greater than unity due to entropy production. The scaled shear-viscous stress tensor starts from zero and approaches the Navier-Stokes limit. Meanwhile, the longitudinal to transverse pressure ratio is given by $\frac{P_L}{P_T} = \frac{\hat{P}-2\hat{\pi}^{xx}}{\hat{P}+\hat{\pi}^{xx}} = 1 - \frac{3\bar{\eta}}{2e_{\bar{\eta}}T_i\tau_i}(\frac{\tau_i}{\hat{x}^0})^{\frac{2}{3}} + \mathcal{O}((\hat{x}^0)^{-\frac{4}{3}})$.

Finally, we are ready to study the proper-time and rapidity dependence of temperature and shear-viscosity by transforming back to the Milne coordinates, $T(\tau, \eta) = \hat{T}(\hat{x}^0(\tau, \eta))$ and $\pi^{xx}(\tau, \eta) = \hat{\pi}^{xx}(\hat{x}^0(\tau, \eta))$. In Fig. 2, we show the rapidity dependence of shear viscous tensor and the difference between the temperature and the corresponding long-time ideal hydro limit, $\Delta T \equiv |\hat{T} - e_{\bar{\eta}}\hat{T}_{\text{ideal}}|$. We have set the overlap time $t_0 = 0.01$ fm/c as in [41]. In a particular η slice, the solution is approaching an ideal hydro limit when proper time increase: values of both π^{xx} and ΔT are getting smaller in τ. π^{xx} is also approaching the Navier-Stokes solution, $\pi^{xx} = \frac{2\bar{\eta}s}{3\hat{x}^0(\tau,\eta)}$, as indicated by the dashed curves. When τ is fixed, the deviations from ideal limit are smaller at larger $|\eta|$. Nevertheless, this does not imply faster relaxation in the larger rapidity region. The larger rapidity region has been initialized with smaller deviation from the long-time limit. To check the speed of relaxation, we may take the ratio between the time evolving values and their corresponding initial values, i.e., $\pi^{xx}(\tau, \eta)/\pi^{xx}(\tau_i, \eta)$ and $\Delta T(\tau, \eta)/\Delta T(\tau_i, \eta)$. Such ratios are shown in the lower panels of Fig. 2. We observe that, at large enough propertime, the ratios are smaller at midrapidity, which indicates faster relaxation. This is consistent with the fact that temperature is higher in the midrapidity region, which means a smaller relaxation time.

Summary and outlook. In this work, we derive new analytical solutions to the Boltzmann equation, which take the relaxation time approximation for the collisions kernel, associated with a newly discovered exact solution of ideal hydrodynamics [41]. The solution assumes homogeneity in the transverse plane, and allows nontrivial rapidity dependence. This is the first analytical solution of the Boltzmann equation that breaks the boost invariance, to the best of our knowledge. With the distribution function, we further construct the stress tensor and compute the effective temperature and shear viscous stress tensor. We observe that both the temperature and the shear viscous stress tensor relax to the limit of hydrodynamics. We also explicitly show the proper-time and rapidity dependence of the deviation of the temperature and shear viscous tensor from the long-time ideal limit, and
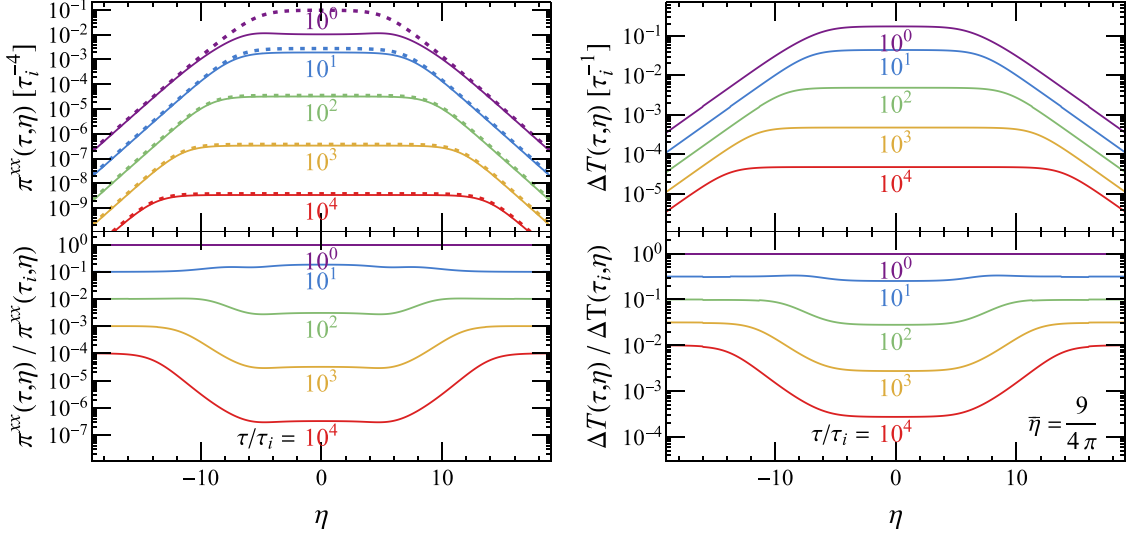
FIG. 2. Rapidity dependence of shear viscous tensor (left) and the difference between the scaled ideal solution the actual temperature (right) at proper time $\tau/\tau_i = 1$(purple), 10(blue), 10^2(green), 10^3(yellow), and 10^4(red). Upper panels are the absolute values whereas lower panels are the ratios between the value at any proper time to those at initial time $\tau = \tau_i$. In the upper left panel, dashed curves are added indicating the Navier–Stokes solution that $\pi^{xx} = \frac{2\bar{\eta}}{3} \frac{s}{\hat{x}^0}$.

we observe faster relaxation at midrapidity, which is higher in temperature. Our solution is useful in testing the applicability and accuracy of different approximations in the derivation of hydrodynamic equations. In particular, if taking the initial distribution in Eq. (12) to be anisotropic in momentum space, one may compare the results with those in anisotropic hydro [44–47]. Results will be reported in future publication.

APPENDIX: LONG-TIME ASYMPTOTIC BEHAVIOR

Here provides Appendix that analyzes the long-time asymptotic behavior (21) of the temperature and shear viscosity self-consistent equations (20) in the main text. For convenience, we use τ to denote the hat proper time $(\hat{x}^0)$ in this Appendix. For later convenience, we define that $F_{\bar{\eta}}(\tau) \equiv \frac{5\bar{\eta}}{e_{\bar{\eta}} T_i \tau_i} (\frac{\tau_i}{\tau})^{\frac{2}{3}}$. We also note that, when $\zeta \to 0$,

$$\tilde{\mathcal{H}}_0(e^{-\zeta}) = \left(1 + \frac{8\zeta^2}{45}\right) e^{-\frac{4}{3}\zeta} + \mathcal{O}(\zeta^3),$$

$$\tilde{\mathcal{H}}_x(e^{-\zeta}) = \frac{8\zeta}{15\pi^2} e^{-\frac{11}{7}\zeta} + \mathcal{O}(\zeta^3). \tag{A1}$$

As the first attempt, we start from solving the "zeroth iteration," putting the ideal solution on the right hand side of

the integral,

$$\hat{T}_{\text{eff},0}^4(\tau) = \frac{1}{5\bar{\eta}} \int_{\tau_i}^{\tau} D_{\text{ideal}}(\tau, t) \tilde{\mathcal{H}}_0(t/\tau) \hat{T}_{\text{ideal}}^5(t) \, dt, \tag{A2}$$

which leads to

$$\hat{T}_{\text{eff}}(\tau) = e_{\bar{\eta}} T_i \left(\frac{\tau_i}{\tau}\right)^{\frac{1}{3}} [1 + \phi F_{\bar{\eta}}(\tau)], \tag{A3}$$

with $e_{\bar{\eta}} = 1$ and $\phi = -\frac{1}{6}$. Such coefficients do not agree with the numerical solution of solving the complete self-consistent equation, but the power of the time dependence is correct. We therefore solve the self-consistent equation for the coefficients. The decay kernel reads

$$D(\tau_2, \tau_1) = \exp\left[-\frac{3}{2F_{\bar{\eta}}(\tau_2)} \left(1 - \left(\frac{\tau_1}{\tau_2}\right)^{\frac{2}{3}}\right)\right] \left(\frac{\tau_1}{\tau_2}\right)^{\phi} \tag{A4}$$

and

$$D(\tau, \tau e^{-\zeta}) = \exp\left[-\frac{3}{2F_{\bar{\eta}}(\tau)}(1 - e^{-\frac{2}{3}\zeta})\right] e^{-\phi\zeta} \tag{A5}$$

$$= \left(1 + \frac{\zeta^2}{3F_{\bar{\eta}}(\tau)} - \frac{2\zeta^3}{27F_{\bar{\eta}}(\tau)} + \frac{\zeta^4}{18F_{\bar{\eta}}^2(\tau)}\right)$$

$$\times e^{-\left(\frac{1}{F_{\bar{\eta}}(\tau)} + \phi\right)\zeta} + \mathcal{O}(\zeta^4). \tag{A6}$$

We replace the integration variable $t = \tau e^{-\zeta}$ in the self-consistent equation (20), and it becomes

$$[1 + \phi F_{\bar{\eta}}(\tau)]^4 = \frac{1}{F_{\bar{\eta}}} \int_0^\infty d\zeta \left(1 + \frac{\zeta^2}{3F_{\bar{\eta}}(\tau)} - \frac{2\zeta^3}{27F_{\bar{\eta}}(\tau)} + \frac{\zeta^4}{18F_{\bar{\eta}}^2(\tau)}\right) e^{-\left(\frac{1}{F_{\bar{\eta}}} + \frac{2}{3} + \phi\right)\zeta} \left(1 + \frac{8\zeta^2}{45}\right) [1 + \phi F_{\bar{\eta}}(\tau)]^5$$

$$= 1 + 4\phi F_{\bar{\eta}}(\tau) + \left(\frac{16}{45} + \frac{8\phi}{3} + 6\phi^2\right) F_{\bar{\eta}}^2(\tau) + \mathcal{O}(F_{\bar{\eta}}^3). \tag{A7}$$

Thus, we find $\phi = -\frac{2}{15}$, and

$$\hat{T}_{\text{eff}}(\tau) = e_{\bar{\eta}} T_i \left(\frac{\tau_i}{\tau}\right)^{\frac{1}{3}} - \frac{2}{3}\frac{\bar{\eta}}{\tau} \frac{\tau_i}{\tau} + \mathcal{O}(\tau^{-\frac{5}{3}}), \tag{A8}$$

Then, computing the long-time behavior of the shear stress tensor become straightforward,

$$\hat{\pi}^{xx}(\tau) = \frac{1}{5\bar{\eta}} \int_{\tau_i}^{\tau} dt\, D(\tau,t)\tilde{\mathcal{H}}_x(t/\tau)\hat{T}_{\text{eff}}^5(t)$$

$$= \frac{8 e_{\bar{\eta}}^4 T_i^4}{15\pi^2}\left(\frac{\tau_i}{\tau}\right)^{\frac{4}{3}} F_{\bar{\eta}}(\tau)\left(1 - \frac{22\, F_{\bar{\eta}}(\tau)}{105}\right) + \mathcal{O}(\tau^{-2}), \tag{A9}$$

so that

$$\frac{\hat{\pi}^{xx}(\tau)\,\tau}{\hat{s}(\tau)} = \frac{2}{3}\bar{\eta} + \frac{40}{63}\frac{\bar{\eta}^2}{e_{\bar{\eta}} T_i \tau_i}\left(\frac{\tau_i}{\tau}\right)^{\frac{2}{3}} + \mathcal{O}(\tau^{-\frac{4}{3}}). \tag{A10}$$

As shown in the main text, such long-time asymptotic formulas are in good agreement with the numerical solution of the self consistent equations (20).

[1] J. Anderson and H. Witting, Physica **74**, 466 (1974).

[2] S. Chapman and T. Cowling, *The Mathematical Theory of Non-uniform Gases: An Account of the Kinetic Theory of Viscosity, Thermal Conduction and Diffusion in Gases*, Cambridge Mathematical Library (Cambridge University Press, Cambridge, 1990).

[3] D. Enskog, Kinetische theorie der vorgänge in mässig verdünnten Gasen., Ph.D. thesis, Fysiska Institutionen, Uppsala Universitet, 1917.

[4] W. Israel and J. M. Stewart, Ann. Phys. (NY) **118**, 341 (1979).

[5] G. S. Denicol, T. Koide, and D. H. Rischke, Phys. Rev. Lett. **105**, 162501 (2010).

[6] G. S. Denicol, H. Niemi, E. Molnar, and D. H. Rischke, Phys. Rev. D **85**, 114047 (2012); **91**, 039902(E) (2015).

[7] G. S. Denicol, S. Jeon, and C. Gale, Phys. Rev. C **90**, 024912 (2014).

[8] P. Romatschke and U. Romatschke, Phys. Rev. Lett. **99**, 172301 (2007).

[9] H. Song and U. W. Heinz, Phys. Rev. C **77**, 064901 (2008).

[10] B. Schenke, S. Jeon, and C. Gale, Phys. Rev. C **82**, 014903 (2010).

[11] W. Zhao, Y. Zhou, K. Murase, and H. Song, Eur. Phys. J. C **80**, 846 (2020).

[12] M. P. Heller, R. A. Janik, and P. Witaszczyk, Phys. Rev. Lett. **108**, 201602 (2012).

[13] M. P. Heller, R. A. Janik, and P. Witaszczyk, Phys. Rev. Lett. **110**, 211602 (2013).

[14] M. P. Heller and M. Spalinski, Phys. Rev. Lett. **115**, 072501 (2015).

[15] A. Kurkela and Y. Zhu, Phys. Rev. Lett. **115**, 182301 (2015).

[16] J.-P. Blaizot and L. Yan, J. High Energ. Phys. 11 (2017) 161.

[17] P. Romatschke, Phys. Rev. Lett. **120**, 012301 (2018).

[18] M. Spaliński, Phys. Lett. B **776**, 468 (2018).

[19] M. Strickland, J. Noronha, and G. S. Denicol, Phys. Rev. D **97**, 036020 (2018).

[20] P. Romatschke, J. High Energ. Phys. 12 (2017) 079.

[21] A. Behtash, C. N. Cruz-Camacho, and M. Martinez, Phys. Rev. D **97**, 044041 (2018).

[22] J.-P. Blaizot and L. Yan, Phys. Lett. B **780**, 283 (2018).

[23] P. Romatschke and U. Romatschke, *Relativistic Fluid Dynamics In and Out of Equilibrium*, Cambridge Monographs on Mathematical Physics (Cambridge University Press, Cambridge, 2019).

[24] A. Kurkela, A. Mazeliauskas, J.-F. Paquet, S. Schlichting, and D. Teaney, Phys. Rev. Lett. **122**, 122302 (2019).

[25] A. Mazeliauskas and J. Berges, Phys. Rev. Lett. **122**, 122301 (2019).

[26] A. Behtash, S. Kamata, M. Martinez, and H. Shi, Phys. Rev. D **99**, 116012 (2019).

[27] U. W. Heinz and J. S. Moreland, J. Phys.: Conf. Ser. **1271**, 012018 (2019).

[28] J.-P. Blaizot and L. Yan, Ann. Phys. (NY) **412**, 167993 (2020).

[29] J.-P. Blaizot and L. Yan, Phys. Lett. B **820**, 136478 (2021).

[30] J.-P. Blaizot and L. Yan, Phys. Rev. C **104**, 055201 (2021).

[31] C. Cercignani and G. M. Kremer, *The Relativistic Boltzmann Equation: Theory and Applications* (Birkhäuser, Basel, 2002), pp. 327–346.

[32] A. Hohenegger, A. Kartavtsev, and M. Lindner, Phys. Rev. D **78**, 085027 (2008).

[33] H. Lee and A. D. Rendall, J. Hyperbolic Differ. Equ. **10**, 77 (2013).

[34] W. Florkowski, R. Ryblewski, and M. Strickland, Phys. Rev. C **88**, 024903 (2013).

[35] W. Florkowski, R. Ryblewski, and M. Strickland, Nucl. Phys. A **916**, 249 (2013).

[36] G. Baym, Phys. Lett. B **138**, 18 (1984).

[37] G. S. Denicol, U. W. Heinz, M. Martinez, J. Noronha, and M. Strickland, Phys. Rev. Lett. **113**, 202301 (2014).

[38] G. S. Denicol, U. W. Heinz, M. Martinez, J. Noronha, and M. Strickland, Phys. Rev. D **90**, 125026 (2014).

[39] M. Strickland, J. High Energ. Phys. 12 (2018) 128.

[40] C. Chattopadhyay, S. Jaiswal, L. Du, U. Heinz, and S. Pal, Phys. Lett. B **824**, 136820 (2022).

[41] S. Shi, S. Jeon, and C. Gale, Phys. Rev. C **105**, L021902 (2022).

[42] R. C. Hwa, Phys. Rev. D **10**, 2260 (1974).

[43] J. D. Bjorken, Phys. Rev. D **27**, 140 (1983).

[44] M. Alqahtani, M. Nopoush, and M. Strickland, Prog. Part. Nucl. Phys. **101**, 204 (2018).

[45] W. Florkowski and R. Ryblewski, Phys. Rev. C **83**, 034907 (2011).

[46] M. Martinez and M. Strickland, Nucl. Phys. A **848**, 183 (2010).

[47] L. Tinti and W. Florkowski, Phys. Rev. C **89**, 034907 (2014).